

Proliferation and DNA Aneuploidy in Mild Dysplasia Imply Early Steps of Cervical Carcinogenesis

Rüdiger G. Steinbeck

From the Department of Tumor Pathology, Karolinska Institute and Hospital, S-171 76 Stockholm, Sweden

Correspondence to: Dr. Rüdiger G. Steinbeck, PO Box 2761, D-24917 Flensburg, Germany, phone: +49 461 5700 173; fax: +49 461 5700 169

Acta Oncologica Vol. 36, No. 1, pp. 3–12, 1997

This project was focused on cellular proliferation relative to the onset of endoreplication and effects of DNA aneuploidy during carcinogenesis in cervical mucosa. Proliferation was monitored with MIB1 antibody, whereas nuclear DNA content was quantified using an image processing microphotometer. For the later procedure, 8 µm sections were of adequate depth with interphases, and lymphocyte nuclei provided an internal standard of the diploid (2c) DNA content. Results from 95 cervical biopsies displaying different types of dysplasia and carcinoma were supplemented with those of cervical smears from 319 cases. The latter specimens had been selected from about 30 000 consecutive cases in 1993/94. MIB1-traced proliferation was found in the second cell layer, whereas the bulk of basal cells remained quiescent in normal mucosa. However, predominant MIB1 immunoreactivity was observed with endoreplicated nuclei. A critical 30% of the cases exhibited DNA aneuploidy already in mild dysplasia, which was found in cytological smears and histological sections. The nuclear DNA content of basal cells increased progressively by endoreplication corresponding to the degree of dysplasia. Cases of carcinoma in situ displayed some 18% of non-proliferating diploid cells despite overwhelming endoreplication and DNA aneuploidy. High MIB1 levels combined with DNA aneuploidy unambiguously indicate the beginning of cervical carcinogenesis. The limits of the Bethesda system were discussed.

Received 28 December 1995

Accepted 10 August 1996

Tumorigenesis in the uterine cervix is suggested to be characterized as a sequence of cellular events caused by genetic alterations. Structural changes caused by the tumorous process provide helpful morphological parameters reflected by the terms mild, moderate and severe dysplasia used in histological diagnosis. Infection with special types of human papilloma virus (1, 2) or malfunctioning tumor suppressor genes are acknowledged examples of interferences with genes regulating the mitotic cell cycle. The molecular damage may cause alterations which can be recognized in smears and microsections. Therefore, it was decided to combine techniques of quantitative microscopy and immunohistochemistry, which are superior in cellular approaches in respect to pure molecular ones. A correlation between cancer and chromosomal aberrations was first considered by Boveri (3). Quantitative histochemistry was used early in pathological diagnosis (4–7), when microphotometry was already applied in analysing precancerous lesions of the cervix. The true cytogenetic aneuploidy was elegantly investigated in cervical carcinogenesis by Granberg (8). Frequent gains and losses of DNA

sequences have been especially observed by comparative genomic hybridization (9). This novel technique hybridizing a mixture of tumor DNA and standard genomic DNA to standard metaphase spreads has made obvious that DNA aneuploidy is not simply equivalent to chromosomal aneuploidy.

Proliferation is usually monitored by antibodies responding towards the proliferating cell nuclear antigen (10) or the Ki67 or MIB1 antigens (11). Recently, it has been shown that the progress of cervical dysplasia is paralleled to enhanced MIB1 immunoreactivity closely following the borderline of nuclear atypia. Non-proliferating cells with mature cytoplasm and diploid nuclei have been found in decreasing numbers from mild and moderate to severe dysplasia (MiD, MoD and SD respectively) in cervical tissue (12). It remained questionable, a) when cellular proliferation and DNA aneuploidy are established and how they relate to each other, b) why some diploid cells can be detected in superficial layers in severe dysplasia, and c) why invasive carcinoma (Ca) might not be detected in smears.

The present paper was devoted to these questions, focusing on the mitotic cell cycle and the onset of genome multiplication (endoreplication). For this purpose, I followed interferences with MIB1 antibody. Development of DNA aneuploidy was monitored by image microphotometry in all cell layers during the course of tumorigenesis. This diagnostic approach seemed useful in pathological routine diagnosis, because squamous epithelium can easily be investigated according to its sequential compartments. Since cytological smears allow insight to the cytoplasm and provide intact nuclei, the technique was used to improve the histological studies. Thus, I followed proliferation and DNA ploidy in stages of cervical pre-neoplasia and cancer in order to understand progression better.

MATERIAL AND METHODS

From about 8 000 cases in 1993 and 22 247 consecutive cases in 1994, 319 cervical smears were selected, displaying different degrees of nuclear atypia. Additionally, 95 cervical biopsies were histologically classified as mild dysplasia (MiD, n = 33), moderate dysplasia (MoD, n = 20), severe dysplasia (SD, n = 24), carcinoma in situ (CIS, n = 8), and carcinoma (Ca, n = 10). Normal mucosa (NM, n = 15) was used as a standard. All patients were from the Flensburg district in Northern Germany and were originally diagnosed at the Institute of Pathology, Flensburg. Approximately 30% of the patients provided both cytological and histological specimens.

Morphological classification

The cytological smears were fixed in 96% ethanol and stained with a modified Papanicolaou technique (13). Dysplasia was primarily classified according to the Munich system II (14); the result was transformed to the CIN system (15, 16). Biopsies were fixed in buffered 4% formaldehyde and were paraffin embedded. For histological diagnosis, the respective WHO rules were applied with 4 µm sections, stained with hematoxilin and eosin (H & E). Further qualitative and quantitative investigations followed the schedule shown in Fig. 1. This procedure guaranteed comparable cell compartments assessing the parameters for DNA content and cellular proliferation.

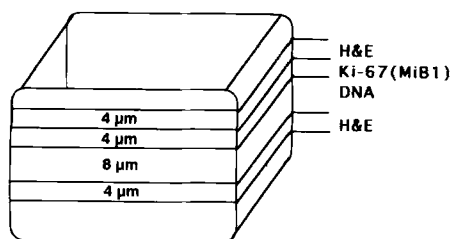


Fig. 1. Paraffin-embedded tissue sample. Microsections for the investigation process.

Quantitative DNA analysis

Reliability of DNA content was improved with microphotometry of 8 µm sections, whereas a depth of only 4 µm frequently was insufficient to cover intact nuclei (Fig. 2). Therefore, 8 µm sections were routinely cut from the paraffin-embedded specimens, then re-hydrated in decreasing grades of ethanol and exposed to hydrolysis using one batch of 5M HCl at 22°C for 60 min. Samples were rinsed in distilled water, stained with one batch of Schiff's reagent at RT for 90 min, and washed in sulfuric acid (10 ml Na₂S₂O₅, 10 ml HCl, 180 ml distilled water; 3x). Finally, they were rinsed in tap water, dehydrated in increasing grades of ethanol, transferred to xylene, and mounted in Eukitt (refractory index 1.494). DNA content of individual cell nuclei was measured at random (ref Fig. 3a) and within selected areas (Fig. 3b–e). In each case, 150 cell nuclei were measured. All specimens were measured by one operator only, using a TV-based and computer-assisted image-analysis system. The measuring microscope (Axioscope; Zeiss) was equipped with a plan-objective (40/0.95 for immersion; Nikon) and a CCD-camera (Nikon). The operator was highly experienced in morphology and provided reliability on four criteria: 1) The correct tumor area, corresponding with the cytological diagnosis, was selected for measurement. 2) Tumor cells were correctly identified in sections. 3) Overlapping nuclei and those which showed degenerated envelopes were excluded. 4) Nuclei which were cut during microsectioning were also avoided. They were identified by focusing up and down and searching for gaps, i.e. spots without contrast on the monitor (Fig. 2). In each case, the mean of at least 20 lymphocyte nuclei provided an internal standard for the diploid (2c) DNA content.

Histogram interpretation

Using image microphotometry, distribution profiles of nuclear DNA content were obtained and assigned accord-

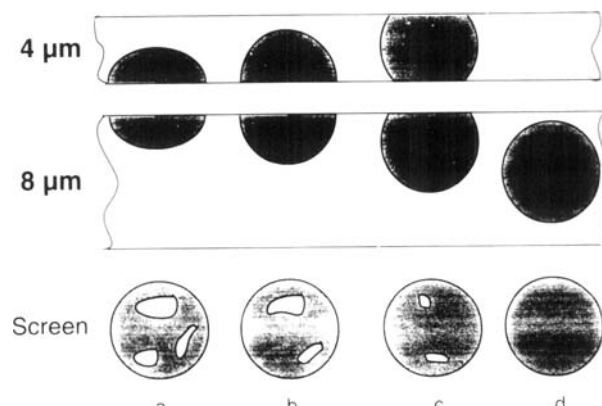


Fig. 2. Effects of 4 µm and 8 µm sections for microphotometry of nuclear DNA. Cut nuclei showed gaps on screen (a–c) and were skipped.

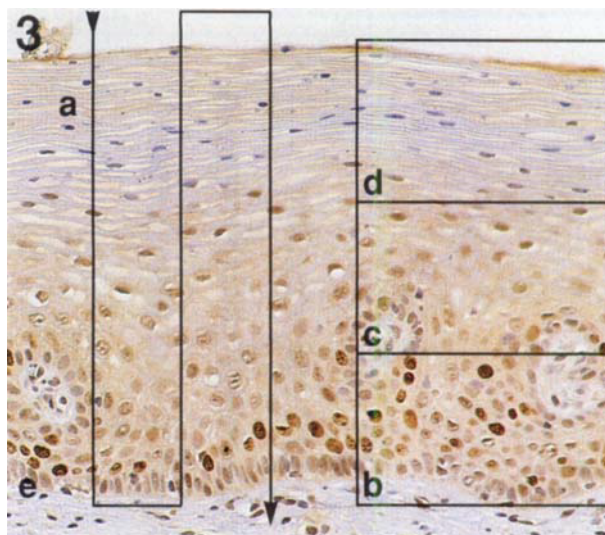


Fig. 3. Nuclear DNA content (profile type I; Fig. 4a) is biased by histological topography, exemplified in normal mucosa: a) random scanning of total cervical epithelium. Selected areas for measurement: b) basal and parabasal cells, c) small intermediate cells, d) large intermediate cells and superficial cells, e) basal cells only. MIB1 reaction with hematoxylin counterstaining.

ing to a modified quantitative method (17). Histograms characterized by a single peak in the diploid region ($1.5c$ – $2.5c$) were classified as type I. The frequency of cells with DNA values exceeding the diploid region ($>2.5c$) was $<10\%$ (Fig. 4a). Type II was regularly found in smears from asymptomatic women, either post-parturient or post-menopausal (Fig. 4b). Type III was characterized by DNA values ranging between the diploid and tetraploid region (main peak at $2.5c$ – $3.5c$). Only a few cells ($<5\%$) remained diploid and others had more than $4.5c$ (Fig. 4c). Type IV showed increased ($>5\%$) values exceeding $4.5c$ by DNA endoreplication. This type comprises cell populations with weakened genomic stability (DNA aneuploidy; Fig. 4d).

Immunohistochemistry

MIB1 antibody (Novocastra, Newcastle upon Tyne, U.K.) was diluted 1:150 with 1% BSA (bovine serum albumin in TPBS = Tris and phosphate buffered saline, pH 7). The formalin-fixed paraffin-embedded $4\ \mu m$ sections, which had been mounted on glass slides and oven-dried for 2 h at $55^{\circ}C$, were deparaffinized in xylene and passed through a graded ethanol series. The slides were transferred to citrate buffer (pH 6) and boiled in a microwave oven at 750 W for 10 min and rinsed in TPBS (11). Then, specimens were immersed for 30 min in 0.6% hydrogen peroxide ($100\ \mu l$ 30% H_2O_2 in 5 ml distilled water) to chase endogenous peroxidase activity. Slides were subsequently washed several times in water and shortly in TPBS and then immersed in 1% BSA for

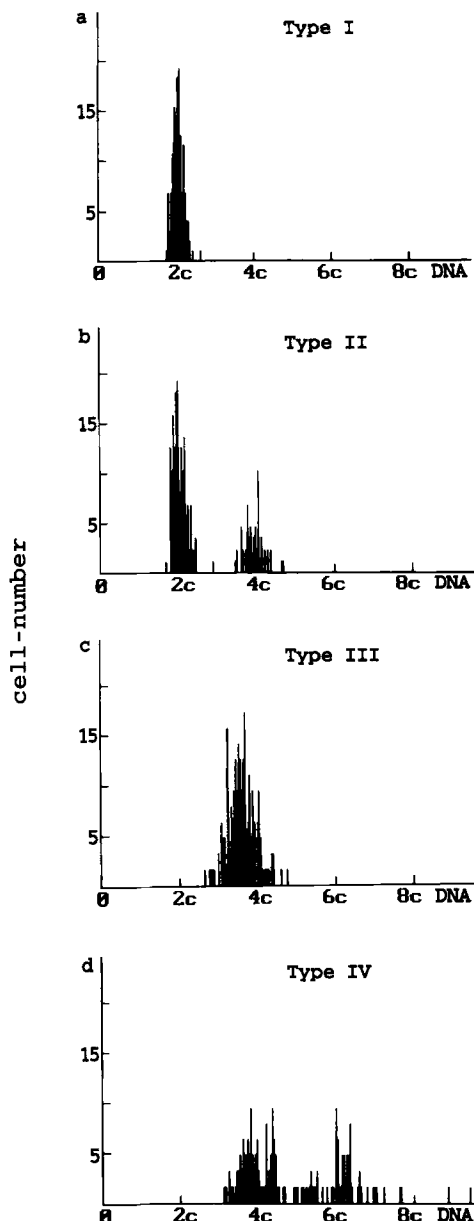


Fig. 4. DNA distribution patterns and their interpretation. Profiles created by microphotometry of 150 cell nuclei in each case. a) Type I: diploid distribution from the case shown in Fig. 3a. b) Type II: a full mitotic distribution ($2c$ – $4c$; Fig. 3b; case shown in Fig. 7). c) Type III: disturbed mitotic cell cycle with low-rate endoreplication (case Fig. 11a). d) Type IV: high-rate endoreplication displaying DNA aneuploidy (case Fig. 11b).

45 min to reduce non-specific antibody binding. Specimens were loaded with the above mentioned antibody dilution, coverslipped and incubated in a humid chamber at $4^{\circ}C$ overnight. After rinsing in three batches of TPBS (5 min each), biotinylated secondary anti-mouse IgG (BA-1000, Vector, Burlingame, U.S.A.; diluted 1:200 in TPBS) was applied at $22^{\circ}C$ for 30–45 min. Subsequently, the specimens were washed in three batches of TPBS (5 min each). ABC solution (Vectastain, Elite ABC Kit; Vector) was

applied for 45 min. After three batches of TPBS (5 min each), diaminobenzidine-hydrogen peroxide (Sigma; 600 μ l DAB stock-solution in 50 ml TPBS, supplemented with 500 μ l 3% H₂O₂) was used as a chromogen. Mayer's hematoxylin solution was applied for light counterstaining. Finally, specimens were dehydrated in ethanol, transferred to xylene and mounted in Pertex (Histolab, Göteborg, Sweden).

Evaluation of immunostained specimens

Only cells with a distinct brown colored staining confined to the nuclei were considered in the MIB1 antibody approach. Immunoreactive cells were counted in morphologically selected areas and recorded as percentage of dysplastic and cancer cells. The lowest number was approximately 2 000 scored cells in each lesion. Histological sections from lymph nodes were used as external positive (central part) and negative (peripheral part) controls.

RESULTS

MIB1 label and DNA content

MIB1 immunoreactivity was evaluated in the whole compartment comprising basal, parabasal, intermediate and superficial squamous epithelial cells set to 100%. From there, the portion of decorated nuclei was estimated in all types of lesions (Fig. 5). MIB1 antigen expression increased through the sequence of dysplasia, ending at a high level with carcinoma. DNA content was recorded within the same compartment where the nuclei were selected at random. Already in MiD, a surprising 30% of the cases showed DNA aneuploidy according to DNA profile type IV. The proportion raised to 100% in SD, as well as in cervical Ca. The borderline between proliferating and non-proliferating nuclei followed sharply the criteria of dysplasia with respect to morphology. In SD, the whole mucous membrane was MIB1 decorated, except for a small superficial rim containing nuclei with condensed chromatin. The progress of dysplasia is paralleled to nuclear MIB1 staining.

Progress of dysplasia

To investigate the compartment of nuclear atypia in all types of lesions, I performed further MIB1 analyses and DNA quantifications including type III and type IV profiles (Fig. 6). For MiD, basal cells and parabasal cell layers were evaluated for both parameters as indicated in Fig. 3b. Since in MoD the small intermediate cells were also MIB1 positive, these cells were included in microphotometry (Fig. 3b, c). Finally, the superficial cells must be added in SD (Fig. 3b, c, d). Thus, the DNA measurements followed the corresponding and increasing MIB1 positive areas which were congruent with the increasing

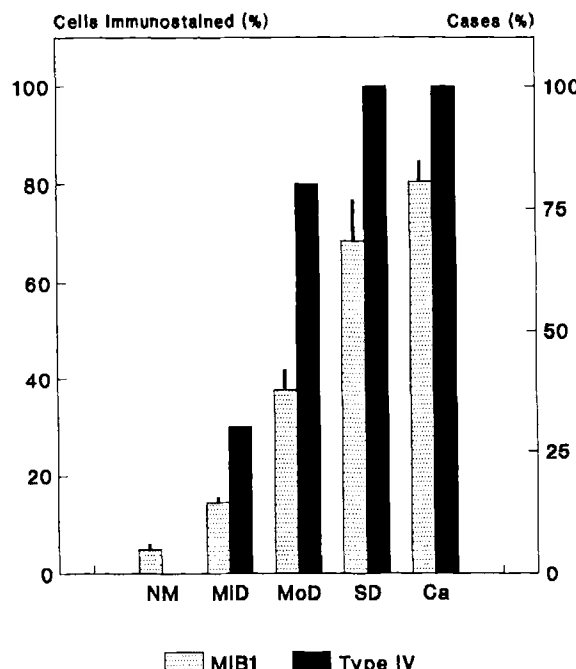


Fig. 5. Cervical epithelium: histology of normal mucosa (NM), mild dysplasia (MiD), moderate dysplasia (MoD), severe dysplasia (SD) and carcinoma (Ca). MIB1 immunoreactivity (+standard error) was compared to occurrence of DNA aneuploidy. For the latter, sections were measured at random (see Fig. 3a). DNA profile type IV was not found in 5 cases of NM, but attained 30% in MiD ($n = 19$), 80% in MoD ($n = 9$), 100% in SD ($n = 7$) and 100% in Ca ($n = 10$).

areas of dysplasia. These analyses, which were based on structure and pathological development of nuclear atypia, revealed that cellular proliferation was paralleled to DNA-profile type III and preceded DNA aneuploidy as obvious from the type IV profile (Fig. 6). It is important that the final development into Ca via SD was exclusively characterized by the type IV profile.

Cervical cytology

The early establishment of DNA aneuploidy was also noticed using a cytological approach. Nuclear microphotometry on cervical smears revealed a significant proportion of DNA aneuploidy in early dysplastic lesions as indicated by a 60.6% type IV profile (Table). Similar to histology, an increase in DNA aneuploidy followed the progress of atypical cells through the whole epithelial compartment. This observation was obvious from 97% type IV in SD (CIN III) and 100% type IV profile in Ca. Smears with doubtful cytomorphological diagnosis contained nuclei detached from their tissue environment. Quantitative discrimination due to DNA content is not easily done with nuclei within the mitotic cell cycle. This task has become feasible with the aid of image microphotometry (Figs. 7, 8). Some doubts remained to those nuclei >2c which still covered the mitotic range of DNA contents, because a 4c

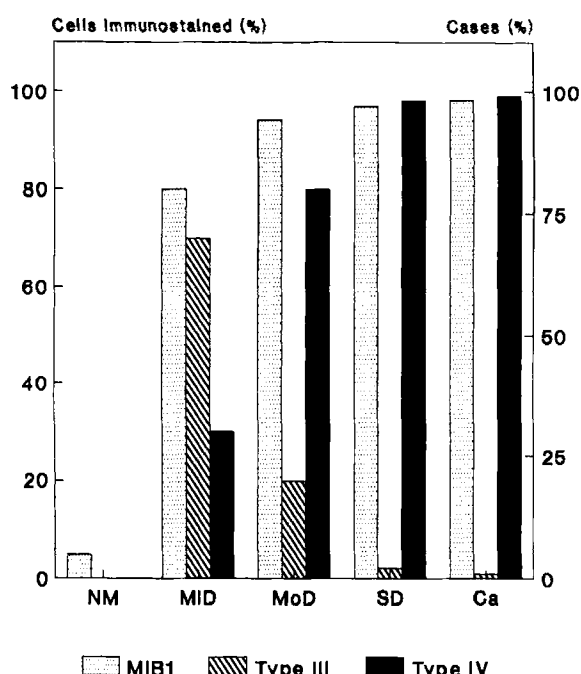


Fig. 6. Selected areas in cervical epithelium of normal mucosa (NM), classified dysplasia, and carcinoma (cases as in Fig. 5). MIB1 immunoreactivity (% of cells) was compared with two DNA profiles, i.e. type III and type IV (% of cases). Areas: for MiD as Fig. 3b, for MoD as Fig. 3b, and c, for SD and Ca as Fig. 3b, c, and d.

nucleus per se does not reveal whether it is prepared for division in mitotic anaphase or has entered the string of

Table

Cytological smears were diagnosed and compared with nuclear DNA content. In total, 319 from estimated 30 000 consecutive cases (1993/1994) were classified according to CIN and microphotometry (16, 17). Only 0.1% of cases were positive for cancer

Cytological diagnosis	Sample (n)	Classification of DNA content		
		I/II	III	IV
Suspicious for CIN	65	55.4%	44.6%	0
CIN I, II	216	5.1%	34.3%	60.6%
CIN III	35	0	2.9%	97.1%
Carcinoma	3	0	0	100%

endoreplications (Fig. 7). However, the mature differentiation of cytoplasm provided an additional, morphological parameter that this cell abandoned the pure mitotic cycle and entered a terminally differentiated status (central cell in Fig. 8). DNA aneuploidy with 1.9c, 4.2c, 5.6c, 5.8c, 7.1c, and 9.2c was recorded also in a cytological smear classified as MiD (CIN I; Fig. 9). The many cases of nuclear atypia in these superficial cells were 'prospectively' diagnosed as MiD. The type of lesion was confirmed in the histological specimen (Fig. 11a,b). The findings were confirmed in a larger sample of n = 319, selected from about 30 000 diagnosed smears in 1993/1994. In the latter sample, 216 cases or 67.7% were classified as type I and type II of cervical intra-epithelial neoplasia (CIN I and CIN II respectively), equivalent to MiD and MoD in the WHO proposal. A fraction of 131 cases (60.6%) showed a type IV DNA profile equivalent to DNA aneuploidy. A further 34.3% exhibited a type III profile indicating severe

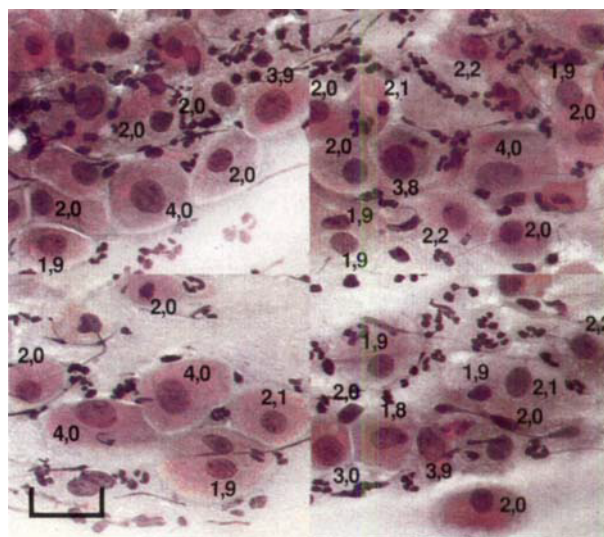


Fig. 7. Smear with atrophic epithelial cells showing DNA profile type II (Fig. 4b). Nuclei in the range 1.9c–4.0c with immature cytoplasm. Calibration for c values was done with lymphocyte nuclei as an internal DNA standard. Papanicolaou prior to Feulgen. Bar represents 25 µm.



Fig. 8. Smear with superficial epithelial cells. Mild dysplasia (CIN I) displaying DNA profile type III. Nuclei in the range 1.9c–4.5c. Papanicolaou prior to Feulgen. Bar represents 25 µm.

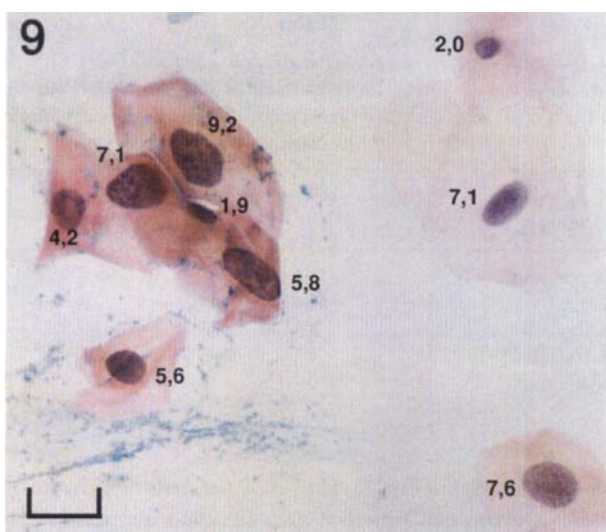


Fig. 9. Mild dysplasia (CIN I) in superficial cells from another case than Fig. 8. Cells from different areas of one Papanicolaou smear. Nuclear Feulgen DNA ranged from 1.9c to 9.2c displaying DNA profile type IV. Bar represents 25 μ m.

disturbances with the mitotic cycle. Interestingly, the three carcinomas were positive for DNA aneuploidy in smears (Table). The same result was obtained from 10 further carcinomas in histological specimens (Fig. 5, 6).

Basal cells

The cell layer of basal cells was earlier believed not only to contain the epithelial stem cells, but also to provide the main proliferative activity in cervical epithelium. The DNA content was quantified from single basal cell nuclei from sections as shown in Material and methods (Fig. 3e). Fifty cases of dysplasia, histologically qualified, were represented by single slides on which 150 basal cells were recorded in fractions of 1.8c–2.4c, 2.5c–4.9c and >5c Feulgen DNA respectively (Fig. 10). In normal mucosa as a rule, the basal cells were diploid (2c). Interestingly, DNA contents reflecting proliferative activity and slight anomalies (2.5c–4.9c), as well as clear DNA aneuploidy (>5c), occupied the basal cell layer with the progress of cervical dysplasia. On the other hand, the number of cells with 1.8c–2.4c DNA range drastically decreased below 20% in carcinoma in situ (CIS).

Mild dysplasia

The qualitative morphology and quantitative characteristics of cervical MiD in cytological smears were documented synoptically with those in histological sections (Figs. 8, 9, 11). CIN I showed nuclear hyperchromasia, pleomorphism and MIB1 reactivity in the basal third of the epithelium. The basal cells were frequently devoid of MIB1 decoration. This finding was in agreement with the

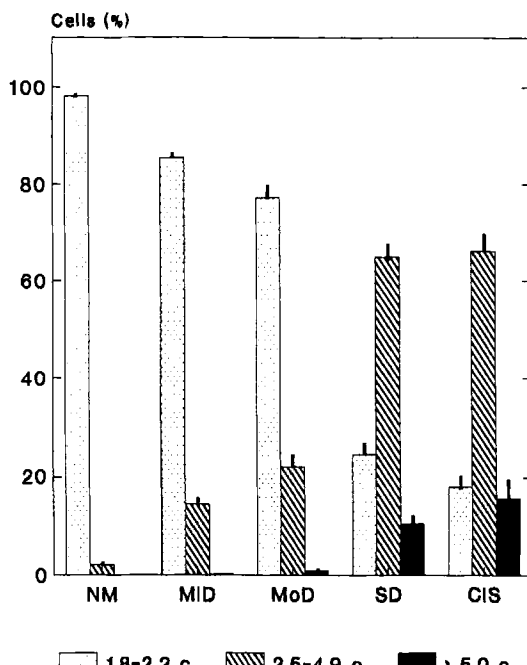


Fig. 10. DNA content of basal cells in different grades of dysplasia and in normal mucosa. Nuclear Feulgen-DNA was quantified in 150 cells on each slide. Area for microphotometry see Fig. 3e. Fractions of 1.8c–2.4c, 2.5c–4.9c and >5c were recorded. NM ($n = 10$ cases), MiD ($n = 14$), MoD ($n = 11$), SD ($n = 17$), and CIS carcinoma in situ ($n = 8$). Abbreviations as Fig. 5. Numerical scatter recorded as standard error.

results previously presented (Fig. 10). Maturation of the cytoplasm occurred in the outer two-thirds. There, the nuclear atypia persisted up to the surface, however without immuno-staining. CIN I type of lesion was found to produce two different types of DNA profiles: 70% of the cases were of type III (Fig. 11a), and 30% were of type IV (Fig. 11b). In addition to the histological findings, it was also possible to cytomorphologically demonstrate the two different types of DNA profile for MiD in cervical smears (Figs. 8, 9). I also felt inclined to document the differences between atrophic smears (Fig. 7) and smears with MiD (CIN I; Fig. 8). The size of cell nuclei was rather similar in both cases, whereas the cytoplasm was immature and mature respectively. Concerning the DNA content, type-II profiles were found in smears after parturition and in smears from atrophic cervical mucosa. Fig. 12 demonstrates that an aneuploid cell population in MiD might develop immediately into cancer without transforming intermediate and superficial cell layers. The example explains how a correct diagnosis with negative record could fail to detect a cancer lesion (thus being a false negative report).

DISCUSSION

Reliability in microphotometry

The differences in nuclear DNA content relevant for cellular classification are hardly detected by simple light mi-

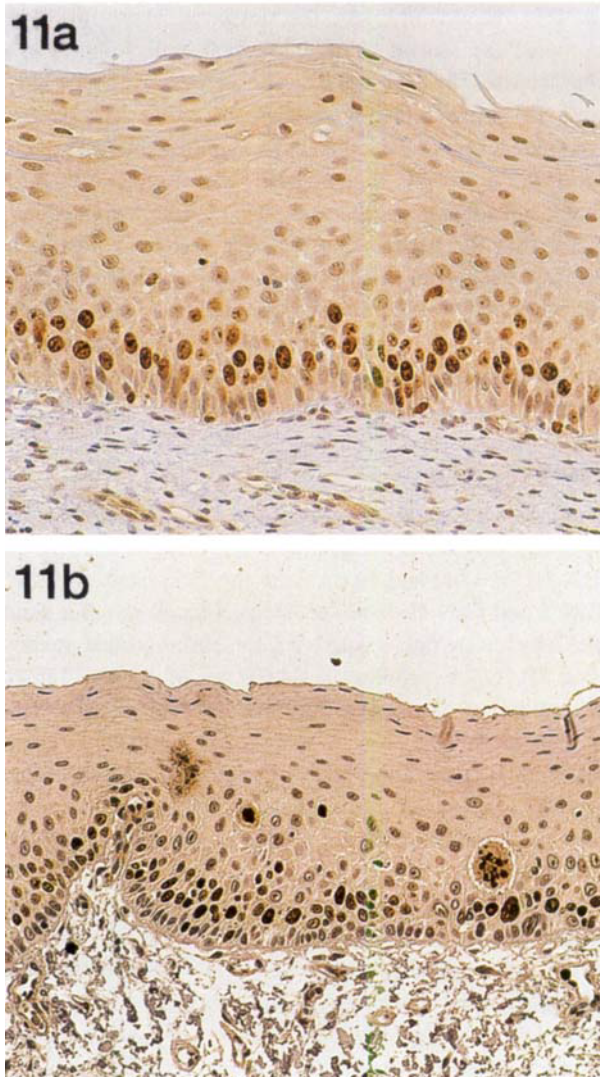


Fig. 11. Histology of mild dysplasia with enhanced MIB1 decoration. a) MiD showing DNA profile type III (Fig. 4c). b) MiD with profile type IV (Fig. 4d).

croscopy. One reason is that nuclear volume and DNA content increase to the power of 3 of the radius. Since a cellular internal standard for optical density is not available for nuclear hyperchromacy, microphotometry is an essential support for diagnostic decisions regarding endoreplication. The vast majority of cell nuclei shows DNA aneuploidy in cervical carcinomas. It is mainly flow fluorometry which has contributed to this view (18, 19). Moreover, (image) microphotometry in histological sections has been hindered by sliced and incomplete cell nuclei. Methodological improvement has been established recently resulting in DNA measurement with high accuracy and reliability (20–22). Nuclear integrity was achieved by sufficient depth of sections; 8 μm was sufficient for interphases up to 8c DNA content in cervical tissue (12). For example, if given the diameter 5.00 μm for



Fig. 12. Histology of cervix carcinoma with early stage of invasion. The tumor developed from basal and parabasal cells which were stained earlier with PC10 antibody for PCNA and were confirmed for DNA aneuploidy. The intermediate superficial cell layers were not transformed as seen from the overview (inlet).

a ball-shaped human 2c nucleus measured in sections, then a diameter of 7.94 μm can be calculated for an 8c nucleus. The latter is within the depth of the sections. These considerations have been proven for high reliability in histological sections and matched imprints of breast carcinoma (Steinbeck RG, Auer GU and Zetterberg A, not published). However, DNA quantitative analysis cannot be used to decide on 4c nuclei which either are prepared for mitotic metaphase and anaphase, or have successfully passed the first endoreplication. Thus, the grade of differentiation in these doubtful cells was established using their cytoplasm, along with their nuclei. Mature cytoplasm (Fig. 8, center) leads to suggest that the cell has abolished the mitotic cycle. It was devoted rather to genome multiplication which stopped shortly after the first endoreplication. Another population of 4c nuclei was found in smears from post-parturient as well as in post-menopausal women with atrophic cervical mucosa (Figs. 4b, 7). The mucous membrane returned to normal (type-I profile; Fig. 4a) after the nursing period in the former instance, or after estrogen application in post-menopausal cases.

Endoreplication and DNA aneuploidy

DNA values clearly above the mitotic range of 2c–4c are brought about by reinitiation of DNA synthesis in the non-dividing nucleus where uncoupling of S-phase and mitosis occurs (23). To detect this process of endoreplication, a threshold has been defined using the 5c exceeding rate for ensured practice. If consecutive DNA syntheses would perform true re-duplications, distribution profiles of nuclear DNA content within geometric 2ⁿ peaks should then result. Such discontinuous DNA profiles were not obtained from cervical epithelia showing dysplastic alterations. In contrast, endoreplicated nuclei produced continuously dispersed profiles which cannot be explained solely by deficient or supernumerary chromosomes. Therefore, the term DNA aneuploidy as been coined (7). Cytogenetically proven aneuploidy has been confirmed with CIS (8). An important question is the source of DNA aneuploidy especially in MiD. Recent investigations indicate that peculiar chromosome division figures in atypical mitoses (CDFs; Fig. 11, right edge) stand for severe genomic imbalance causing aneuploid DNA profiles from precancerous lesions in oral mucosa and in colon adenomas (Steinbeck, in preparation). Atypia in MiD arises in the first generation of daughter cells which is produced by the basal cells. The interpretation is supported by enhanced MIB1 reactivity and anomalies from 2.5c–3.5c DNA content (type III profile, Fig. 4c). These atypical cells did not enter mitosis and appeared after maturation in the superficial layer (histology) and in smears (cytology). Furthermore, the developmental disturbance of MiD induced the first cases of DNA aneuploidy (type IV profile, Fig. 4d) in the adjacent layer distal to the basal cells (Fig. 11a, b). The proper basal cells were generally in the mitotic range and possessed only a minor MIB1 positive fraction in MiD. In consequence, one could hypothesize that the aberrations are caused by somatic modifications or mutations in the gene cascade that regulates the mitotic cell cycle (23, 24). Further research will decide to which extent cytogenetic aneuploidy, especially amplification of chromosome 3q (9), is already present in MiD.

MIB1 interpretation

Reviewing the whole compartment of cervical epithelium, random measurements of nuclear DNA content suggested that DNA aneuploidy in 30% of the MiD cases is accompanied by high and specific MIB1 immunoreactivity in atypical cells (Fig. 5; ref. 11). The relation of morphological lesions and nuclear changes was further analyzed by focusing solely on dysplastic districts. Thus, it was shown that a MIB1 staining frequently paralleled DNA endoreplication. Cells only within the basal third of the epithelium were labeled by MIB1 antibody following closely the criteria of MiD. Of these cells, 70% revealed anomalous nuclear DNA type III, and 30% type IV profi-

les (Fig. 6). In addition, the advanced status of MoD occupied the second third of cervical epithelium. It was characterized by 94% MIB1 positive cells with prevalent type IV profile. The final steps of carcinogenesis had conquered the whole epithelial compartment (CIS), and cervical Ca showed a high MIB1 decoration as well as DNA aneuploidy in all cases. The results provided evidence that the MIB1 antigen rather became expressed in cervical cells engaged in endoreplication, while only in a few cells devoted to mitotic proliferation (cell number multiplication). This multivalence of MIB1 antibody demands urgent clearing up of the molecular nature of the corresponding antigen and that of Ki67.

Tumor progression

The cytologic results underlined the findings from cervical histology that DNA aneuploidy is an early event; 97.1% of CIN III (n = 35) and 60.6% from the 216 smears classified CIN I and CIN II exhibited DNA aneuploidy. But samples which were only suspected CIN, had exhibited already type III DNA profiles in 44.6% of 65 cases (Table). According to the above interpretation, these cells were starting endoreplication in MiD to establish DNA aneuploidy or entering apoptosis. This situation was illustrated by a 4.5c nucleus of a smear (Fig. 8, center) and a mature superficial epithelial cell containing a diploid nucleus (Fig. 8, right).

By definition, MiD shows nuclear atypia and deficient differentiation only in the basal layers of the mucosa. These cells met with mutation(s) which prevent passage through mitosis and differentiation in time. Endoreplication, DNA aneuploidy and CDFs are further consequences. When endoreplication comes to an end, delayed cytoplasmic differentiation is allowed. How do these somatic genetic alterations fail to be noticed with light microscopy in the superficial stratum? Some of the atypical cells will die entering apoptosis before reaching the surface. Others, not mentioned in the histological MiD classification defined by the WHO, will reach the superficial layer becoming available to the smear technique. But most of the superficial cells were found at 2c, i.e. in the quiescent Go period (Figs 8, 9). The putative paradox of MiD is solved by the straight forward interpretation that mitotic cells are not only privileged by numerical proliferation, but are favoured by also enhanced growth. Thus, cells with endoreplicated nuclei have to stay longer in the basal cell compartment. The stratigraphy of MiD is not only found in small lesions but is also present in extensive lesions. The latter finding demonstrates that it is unlikely that MiD would be covered by normal epithelium spreading laterally from surrounding mucosa. It is more convenient that those basal cells which remained genetically stable produced the superficial layer. Progression towards more serious lesions is scarcely an effect of less over-

growth. Transition from SD to Ca is rather caused by unrestricted somatic mutations allowing high-rate endoreplication with DNA aneuploidy, thus reducing the source of diploid cells in the basal compartment (Fig. 10). The process may generate different clones of malignant (mitotic) cells.

It has been concluded that deregulations detected by nuclear atypia at the outer surface of cervical epithelium indicate low risk for the patient if normal basal cells do persist. This hypothesis gains support from the fact that MiD, MoD and (in few instances) SD underwent regression. The potential cause for such events are unidentified stem cells at the basement membrane. Indeed, a subpopulation of 20% diploid cells was found at the basement membrane with 30% cases of SD and CIS, within the bulk of abnormal cells (Figs. 10, 11b). Therefore, it was not a surprise that some 2c nuclei were still observed at the outer epithelial surface in SD. The findings of DNA aneuploidy in MoD or SD and the report of 3q trisomies in CIS (9) are in agreement with the Bethesda system (25, 26), which qualifies MoD, SD and CIS as high risk lesions on morphological criteria. However, this diagnostic system fails to uncover high risk when DNA aneuploidy already occurs in MiD, which is solely realized by microphotometry. Since some types of the human papilloma virus (e.g. HPV 16) are a main source for endoreplication and DNA aneuploidy, any cervical dysplasia requires additional HPV test.

According to observed frequencies, invasive cancer usually is preceded by MiD, MoD and SD in sequence. But undoubted observations recorded some 5% cervical carcinomas which develop directly from the basal and parabasal cell layer while transformation of intermediate and superficial cells does not occur (Fig. 12). The oral mucosa shows this phenomenon rather frequently (27) corresponding well with the fact that many cases had been diagnosed as falsely negative by oral cytology. Similarly, most primary cutaneous malignant melanomas are known for different patterns of development. The monophasic growth has no superficial epidermal component, but proliferating melanocytes invade directly into the dermis (28). Therefore, the hypothesis is proposed that transformation allowing invasive cell growth is a genetic event not necessarily dependent on factors leading to dysplasia.

ACKNOWLEDGEMENTS

Prof. Gert Auer, Department of Pathology, Karolinska Institutet, Stockholm, has provided part of research facilities. Ms. Ulla Aspenblad, Stockholm, and Mr. Uwe Köster, Flensburg, have given excellent technical assistance. Ms. Andrea Lorenzetti, Bad Iburg, Germany, provided linguistic aids. This study was supported by the Swedish Cancer Society of Stockholm, the King Gustav V Jubilee Fund, the Research Funds of the Faculty of Medicine at the Karolinska Institute, Stockholm (Sweden), and the Research Funds of the Institute of Pathology, Flensburg (Germany).

REFERENCES

- Zur Hausen H. Human papillomaviruses and their possible role in squamous cell carcinomas. *Curr Top Microbiol Immunol* 1977; 78: 1–30.
- Zur Hausen H. Papillomaviruses in human cancer. *Cancer* 1987; 59: 1692–6.
- Boveri T. Zur Frage der Entstehung maligner Tumoren. Jena: Gustav Fischer, 1914.
- Atkin NB, Richards BM. Deoxyribonucleic acid in human tumors as measured by microspectrophotometry of Feulgen stain: A comparison of tumors arising at different sites. *Br J Cancer* 1956; 10: 769–86.
- Caspersson O. Quantitative cytochemical studies on normal, malignant, premalignant and atypical cell populations from the human uterine cervix. *Acta Cytol* 1964; 8: 45–60.
- Wied GL, Messina AM, Meier P, Blough RR. Fluorospectrophotometric analysis on cervical epithelial cells. *Acta Cytol* 1964; 8: 61–7.
- Sandritter W. Methods and results in quantitative cytochemistry. In: Wied GL, ed. *Introduction to quantitative cytochemistry* (vol 1). New York: Academic Press, 1966: 159–82.
- Granberg I. Chromosomes in preinvasive, microinvasive and invasive cervical carcinoma. *Hereditas* 1971; 68: 165–218.
- Heselmeyer K, Schröck E, Du Manoir S, et al. Gain of chromosome 3q defines the transition from severe dysplasia to invasive carcinoma of the uterine cervix. *Proc Natl Acad Sci USA* 1996; 93: 479–84.
- Hall PA, Leivonen DA, Woods AL, et al. Proliferating cell nuclear antigen (PCNA) immunolocalization in paraffin sections as an index of cell proliferation with evidence of deregulated expression in some neoplasms. *J Pathol* 1990; 162: 285–94.
- Cattoretti G, Becker MHG, Key G, et al. Monoclonal antibodies against recombinant parts of the Ki-67 antigen (MIB-1 and MIB-3) detect proliferating cells in microwave-processed formalin-fixed paraffin sections. *J Pathol* 1992; 168: 357–63.
- Steinbeck RG, Heselmeyer KM, Moberger HB, Auer GU. The relationship between proliferating cell nuclear antigen (PCNA), nuclear DNA content and mutant p53 during genesis of cervical carcinoma. *Acta Oncol* 1995; 34: 171–5.
- Papanicolaou GN. A new procedure for staining vaginal smears. *Science* 1942; 95: 438–9.
- Soost H-J. Befundwiedergabe in der gynäkologischen Zytodiagnostik: Münchner Nomenklatur, II. *Gynäkol Prax* 1990; 14: 433–8.
- Naujoks HF, Köpf F, Leber J. Präoperative kolposkopisch-zytologische Diagnostik bei zervikaler intraepithelialer Neoplasie (CIN). *Geburtsh Frauenheilk* 1979; 39: 372–7.
- Richart RM. A modified terminology for cervical intra-epithelial neoplasia. *Obstet Gynecol* 1990; 75: 131–3.
- Auer G, Caspersson T, Wallgren A. DNA content and survival in mammary carcinoma. *Quant Cytol* 1980; 2: 161–5.
- Jelen I, Valente PT, Gautreaux L, Clark GM. Deoxyribonucleic acid ploidy and S-phase fraction are not significant prognostic factors for patient with cervical cancer. *Am J Obstet Gynecol* 1994; 171: 1511–8.
- Kimmig R, Kapsner T, Spelsberg H, Untch M, Hepp H. DNA cell-cycle analysis of cervical cancer by flow cytometry using simultaneous cytokeratin labelling for identification of tumor cells. *J Cancer Res Clin Oncol* 1995; 121: 107–14.
- Moberger B. DNA content and prognosis in endometrial carcinoma. PhD Thesis. Stockholm: Karolinska Institute, 1989.

21. Ghali VS, Liau S, Teplitz C, Prudente R. A comparative study of DNA ploidy in 115 fresh-frozen breast carcinomas by image analysis versus flow cytometry. *Cancer* 1992; 70: 2668–72.
22. Borgiani L, Cogorno P, Toso F, et al. Comparative DNA analysis of breast cancer by flow cytometry and image analysis. *Pathologica* 1994; 86: 356–9.
23. Waldmann T, Lengauer C, Kinzler KW, Vogelstein B. Uncoupling of S phase and mitosis induced by anticancer agents in cells lacking p21. *Nature* 1996; 381: 713–6.
24. Sauer K, Knoblich JA, Richardson H, Lehner CF. Distinct modes of cyclin E/cdc2c kinase regulation and S-phase control in mitotic and endoreduplication cycles of Drosophila embryogenesis. *Genes Development* 1995; 9: 1327–39.
25. Solomon D. The 1988 Bethesda system for reporting cervical/vaginal cytological diagnoses. *Acta Cytol* 1989; 33: 567–74.
26. Solomon D. The revised Bethesda system for reporting cervical/vaginal cytologic diagnoses: Report of the 1991 Bethesda workshop. *Acta Cytol* 1992; 36: 273–6.
27. Steinbeck RG, Moege J, Heselmeyer KM, et al. DNA content and PCNA immunoreactivity in oral precancerous and cancerous lesions. *Oral Oncol Eur J Cancer* 1993; 29 B: 279–84.
28. Mihm Jr MC, Lopansri S. A review of the classification of malignant melanoma. *J Dermatol* 1979; 6: 131–42.